論文の内容の要旨

Materials Exploration and Reaction Mechanism Analyses of Iron-based Cathode Materials for Rechargeable Batteries

（二次電池用鉄系正極の材料探索と反応機構解析）

氏名　大山　剛輔

General introduction

Rechargeable batteries, which power a wide range of applications, are indispensable in our modern lives. Due to the increase in the area of applications, the demands for rechargeable batteries multiplies and becomes more diverse. To satisfy these demands, it is of key importance to develop battery technology with a holistic view. State-of-the-art lithium-ion batteries exhibit excellent performance among all the rechargeable batteries with regard to four dominant parameters: gravimetric/volumetric energy density, cycle life, coulombic efficiency and power density. However, stricter restrictions are imposed not only for the electrode performance parameters listed above, but also for safety and cost; among which the cost is a major obstacle, especially for large-scale applications.

One of the most promising strategies to reduce the material cost is the utilization of iron, which is the fourth most abundant in the earth's crust and an environmentally benign element. In the present thesis, the possibilities of iron based compounds has been pursued through two important classes of cathode materials, olivine lithium iron phosphate, and alluaudite sodium iron sulfate. In part I, kinetics of olivine lithium iron phosphate Li_xFePO_4 and the possibility as a magnesium battery cathode have been surveyed. In part II, a new 3.8 V class sodium-ion battery cathode material, alluaudite sodium iron sulfate is targeted.

Part I Electrochemical behaviors of Olivine Lithium Iron Phosphate

Olivine-type lithium iron phosphate, Li_xFePO_4, is still gaining momentum as one of the most promising cathode materials for large-scale lithium-ion batteries. Owing to the superior kinetics of Li_xFePO_4, the electrochemical reaction mechanism has been an intensive research topic. One-dimensional lithium migration along the *b* direction in Li_xFePO_4 occurs cooperatively to form 2D phase boundary along the *bc* plane, which subsequently move along *a*-axis, described as "Domino-Cascade" model.[1]

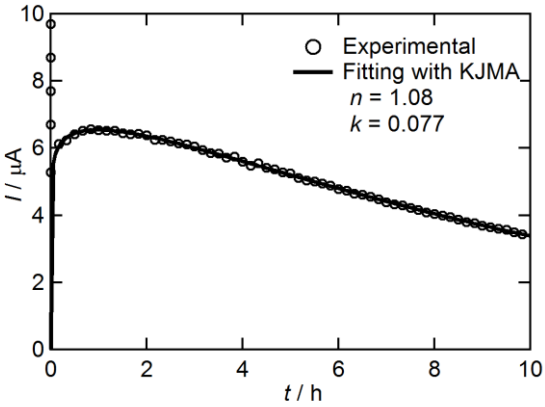

Fig. 1 Chronoamperogram obtained for the $LiFePO_4$ electrode under a 10 mV anodic step. The plots and line denote the experimental and simulating curves. Obtained Avrami exponent (*n*) and rate constant of phase-boundary movement (*k*) are presented.

Here, the kinetics of the phase boundary movement in Li_xFePO_4 are focused. In order to make quantitative analyses of the phase boundary movement in a Li_xFePO_4 composite electrode, we need to set it as being dominant and rate limiting reaction, minimizing the influence of other processes. Towards this end, several conditions (particle size, electrode thickness, step-width of applied voltage, etc.) are tried in order to spotlight the single-particle reaction. Under the optimized condition in which the phase boundary movement is dominant reaction, characteristic current-response profiles in the chronoamperograms are analyzed using KJMA equation (Fig. 1). Obtained Avrami exponent of ca. 1.1 indicates that the phase transition proceeds with

one-dimensional phase-boundary movement, which is consistent with previously reported mechanism. In both lithium-ion intercalation/deintercalation reactions, the activation energy for the phase boundary movement in Li_xFePO_4 is calculated to be ca. 400 meV. The obtained activation energies of phase-boundary movement in Li_xFePO_4 are substantially lower than other processes (e.g. atomic-scale Li diffusion coupled with electron transport). The comparatively small activation energy of phase-boundary movement might be one of the reasons for high rate performance of Li_xFePO_4 electrodes despite their two-phase character.

Utilization of divalent Mg^{2+} is one of the possible ways to exceed theoretical energy density of the current lithium-ion battery systems. In magnesium batteries, magnesium metal can be applicable as an anode (theoretical capacity: 2205 $mAhg^{-1}$), because it does not favor dendritic morphology unlike lithium. Therefore, very large specific capacity can be expected for "magnesium batteries". However, exploring reversible Mg^{2+} (de)intercalation compounds are key issue toward suitable cathode materials for rechargeable magnesium batteries. An intrinsic obstacle for reversible Mg^{2+} (de)intercalation is large deformation of the local structure by accommodation of two-electron associated with Mg^{2+}. For example, the Chevrel phase Mo_6T_8 (T = S and Se) shows fast and reversible Mg^{2+} intercalation, because up to four electrons can be accommodated with delocalized orbital of a Mo_6 cluster.[2] However, the reversible capacity is intrinsically rather limited due to its charge compensation mechanism.

In order to achieve a superior energy density, the electrochemical properties of $FePO_4$ with rigid skeleton framework to accommodate Mg^{2+} are surveyed in aqueous Mg^{2+} electrolyte. The charge/discharge experiments show that $FePO_4$ delivers the first discharge capacity of 90 mAh g^{-1} with subsequent partial reversibility (Fig. 2). The ex-situ Mössbauer spectroscopy measurements confirm that both the amount of Mg^{2+} and corresponding Fe^{3+}/Fe^{2+} redox reversibly change during the discharge and subsequent charge processes. About 50 % of Fe^{3+} in the pristine $FePO_4$ is reduced to Fe^{2+} by discharging, which is in good agreement with the initial discharge capacity of 90.5 mAh g^{-1}. However, little change is observed in the ex-situ X-ray diffraction patterns. It is postulated that the electrochemical reaction of $FePO_4$ in aqueous Mg^{2+} electrolyte is non-topochemical Mg^{2+} (de)intercalation accompanied by the irreversible transformation from the crystalline state to the amorphous state.

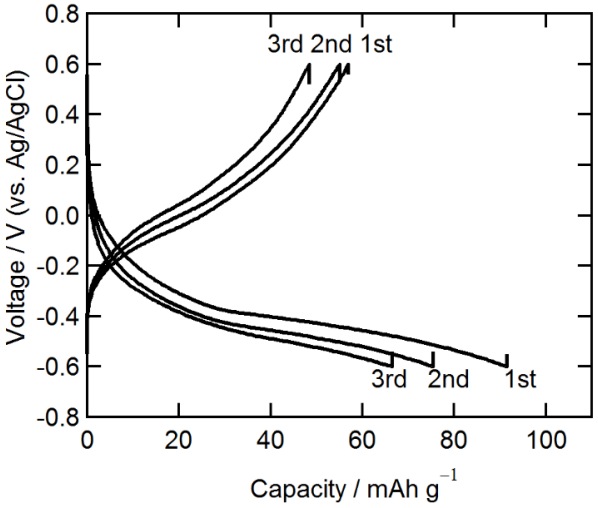

Fig. 2 Discharge/charge curves of $FePO_4$ in 1 mol dm^{-3} $MgSO_4$ aqueous solution at a rate of C/20 (conducting at 298 K).

Part II Alluaudite sodium iron sulfate as a sodium-ion battery cathode

As one of the most realistic alternatives for lithium-ion batteries, sodium-ion batteries re-attract massive attention owing to its abundance, lower cost, and sustainable production. Cathode materials for sodium-ion batteries are under investigation for those consisting of low cost transition metals such as P2-$Na_xMn_{0.5}Fe_{0.5}O_2$, O3-$NaFe_{0.5}Ni_{0.5}O_2$, Na_2FePO_4F, and $Na_2FeP_2O_7$.[3–6] Especially for large-scale applications, iron is an ideal redox center due to its environmental abundance and benignity. However, the Fe^{3+}/Fe^{2+} redox potential in the sodium system is generally too low (< 3 V) to achieve high energy density. One of the established ways to enhance the potential further is to utilize the

inductive effect in oxyanionic compounds. Especially, SO_4^{2-} units take advantage of the strong inductive effect due to high electron negativity of S. Moreover, sulfate compounds are cheap, being a byproduct of coal power plant, or petrochemical industries.

In this pursuit, Na-Fe-S-O systems are one of the most desirable systems, which are consisted only by earth-abundant and geographically distributed elements.

Here, a hitherto-unknown material with the first alluaudite-type sulfate framework, $Na_{2+2x}Fe_{2-x}(SO_4)_3$ are discovered. Through the exploration in the Na_2SO_4-$FeSO_4$ binary system, the compositional range of the solid solution $Na_{2+2x}Fe_{2-x}(SO_4)_3$ is revealed as off-stoichiometric (x = 0.25–0.3). Crystal structure of this new cathode material was determined by direct space method and subsequent Rietveld refinement for a high resolution XRD pattern. Figure 3 shows the crystal structure of the new compound, which is essentially isostructural with a common alkaline manganese iron phosphate mineral, alluaudite. According to a general formula of $AA'BM_2(XO_4)_3$, this compound corresponds to A = Na2, A' = Na3, B = Na1, M = Fe and X = S.

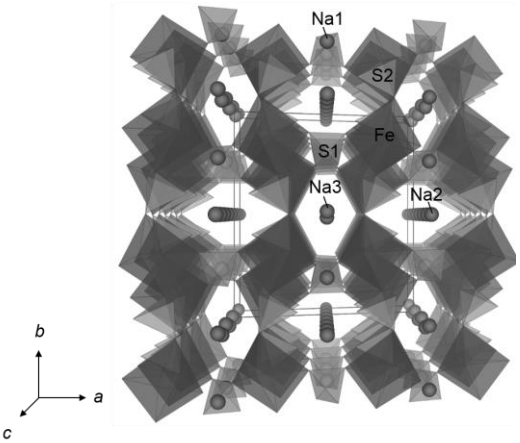

Fig. 3 The crystal structure of alluaudite-type sodium iron sulfate projected along the *c* axis.

Figure 4 shows the corresponding voltage-capacity profiles for the first few cycles. The cathode offers an average potential of 3.8 V (vs. Na/Na^+), which is the highest-ever Fe^{3+}/Fe^{2+} redox potential in any coordination environments. The initial reversible capacity (ca. 100 $mAhg^{-1}$) is highly reversible over 30 cycles under various current rate (Fig. 5). When the current is further increased, 86 % (versus the value at C/20) of the initial capacity can be delivered in 1 h (1C), 85 % in 30 min (2C), and 70 % in 6 min (10C) as shown in Fig. 5.

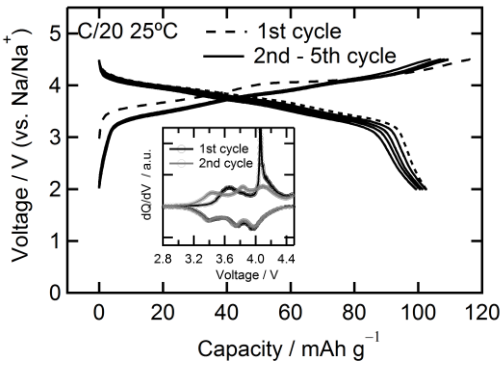

Fig. 4 Voltage-capacity profiles of $Na_{2+2x}Fe_{2-x}(SO_4)_3$ cathode cycled between 2.0 and 4.5 V at a rate of C/20 at 25 °C. **(Inset)** The corresponding dQ/dV curves at the first two cycles.

Then, the electrochemical reaction mechanism of $Na_{2+2x}Fe_{2-x}(SO_4)_3$ are studied via a combined approach with diffraction and spectroscopic measurements. Both ex situ and in situ XRD shows the single-phase (solid-solution) reaction occurred involving the irreversible reaction upon the first charging process.

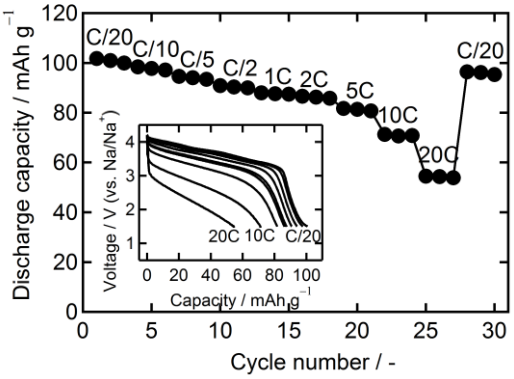

Fig. 5 Capacity retention upon cycling up to 30 cycles under various rate of C/20 to 20C. **(Inset)** The corresponding discharge curves of $Na_{2+2x}Fe_{2-x}(SO_4)_3$ as a function of rate.

The origin of the irreversibility is the Na extraction from Na1 site accompanied by Fe migration from Fe1 to Na1 site, where the driving force can be the strong Fe^{3+}–Fe^{3+} Coulombic repulsion in a short distance within the edge-sharing dimer. This structural rearrangement is only observed upon the first charging process and the structural and Fe^{3+}/Fe^{2+} redox reversibility is retained upon the subsequent cycles with a small volume change (ΔV = ca. 3.5 %), which may contributes to the good cyclability of the electrochemical processes.

Upon the first charge process, sodium extraction primarily occurs at Na3, which is consistent with the computational results for the shallowest potential of the Na3 site, involving the small migration energy between Na3-Na3 sites (<300 meV). Upon the further charging process, sodium are extracted at Na2, and then Na1 sites for the initial charging. The sodium insertion occurred at Na2, Na3, and Na/Fe1 sites for the first discharging, and in the subsequent reversible cycles (Fig. 6). On the other hand, the electronic state of iron reversibly changes even at the irreversible first charging process, suggesting Fe on Fe/Na1 site, participates in redox reaction even after the Fe^{3+} migration.

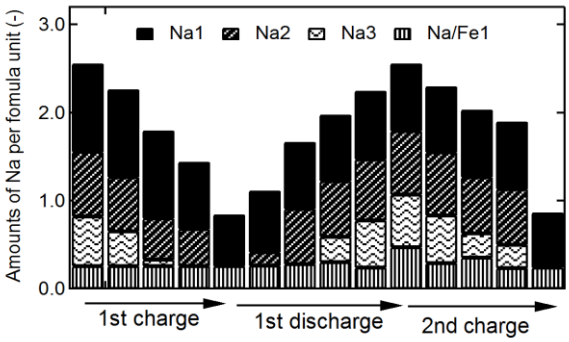

Fig. 6 Amounts of sodium per formula unit in $Na_{2+2x}Fe_{2-x}(SO_4)_3$ during the charge/ discharge processes.

The electronic structure of the $Na_{2+2x}Fe_{2-x}(SO_4)_3$ sulfate is surveyed by combining soft X-ray absorption spectroscopy (XAS), and DFT calculations. Iron *L*-edge spectra shows the Fe 3*d* orbitals are greatly localized under the minimal hybridization with oxygen 2*p* orbitals due to the Fe–O–S inductive effect. The hybridization between Fe–O orbitals enhances upon the desodiation process, and it reversibly weakens upon the subsequent sodiation process, which are due to the shorter Fe–O bond length and the smaller energy gap between Fe and oxygen conduction bands.

Conclusion

In summary, kinetics of the two-phase electrode reaction of Li_xFePO_4 and the electrochemical properties of $FePO_4$ as a magnesium battery cathode have been clarified in part I. The revealed reaction mechanism can contribute to further optimization of the electrode both in lithium-ion and magnesium batteries.

In part II, the composition, structure, electrode performance, reaction mechanism and electronic structure of a new alluaudite-type sodium iron sulfate have been elucidated. The new material $Na_{2+2x}Fe_{2-x}(SO_4)_3$ is benchmarking as it is the first iron-based cathode for sodium-ion batteries to offer high-voltage compatible with lithium-ion batteries (Fig. 7). Rare-metal-free sodium-ion battery system is now in realistic scope without sacrificing high energy and power densities.

The author strongly believes the present study contributes to our basic understanding for iron-based cathodes, and makes a path clearer for discovery of new "earth-abundant" cathode materials for next generation rechargeable batteries in future.

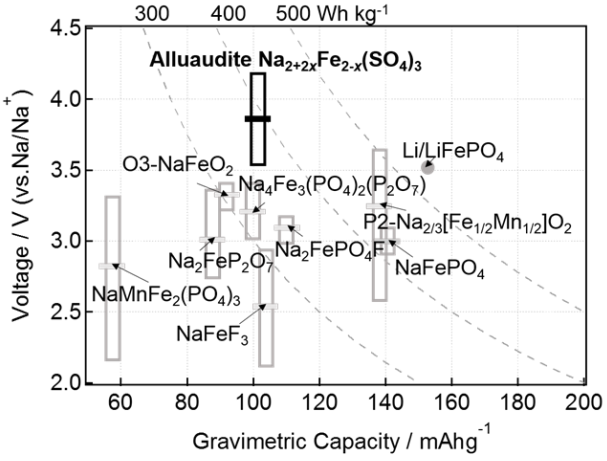

Fig. 7 Overall comparison of the Fe-based cathode materials which can function as sodium sources in Na-ion battery system.

References

(1) Delmas, C. *et al. Nat. Mater.* **2008**, *7*, 665.

(2) Aurbach, D. *et al. Nature* **2000**, *407*, 724.

(3) Yabuuchi, N. *et al. Nat. Mater.* **2012**, *11*, 512.

(4) Wang, X.; *et al. J. Phys. Chem. C* **2014**, *118*, 2970.

(5) Ellis, B. *et al. Nat. Mater.* **2007**, *6*, 749.

(6) Barpanda, P. *et al. Electrochem. commun.* **2012**, *24*, 116.